Coordination Patterns for Biliverdin-Type Ligands. Helical and Linked Helical Units in Four-Coordinate Cobalt and Five-Coordinate Manganese(III) Complexes of Octaethylbilindione

Alan L. Balch,* Marinella Mazzanti, Bruce C. Noll, and Marilyn M. Olmstead

Contribution from the Department of Chemistry, University of California, Davis, California 95616

*Received November 10, 1993. Revised Manuscript Received June 9, 1994**

Abstract: The bilindione tetrapyrrole unit that is found in biliverdin, an intermediate in heme catabolism, is widely distributed in nature especially as a pigment, but its ability to act as a ligand toward metal ions and the range of complexes that it can form have received little attention. Because of the presence of the two keto groups at opposite ends, this type of tetrapyrrole cannot readily form planar structures analogous to those of porphyrins. Rather this tetrapyrrole ligand adopts a helical arrangement that minimizes contact between its terminal keto groups. Three complexes, monomeric {(OEB)Co}, dimeric $\{(OEB)Mn^{III}\}_2$, and monomeric {(OEB)Mn^{III}(py)} of octaethylbilindione (H_3OEB), have been characterized by X-ray diffraction and spectroscopic techniques. The cobalt complex consists of a cobalt ion with approximately planar coordination that is surrounded by four pyrrole nitrogen atoms of the helical ligand. The ^1H NMR spectrum has marked temperature dependent changes. These changes are most prominent in the meso resonances and indicate that there is thermal population of a low-lying paramagnetic state. This behavior may result from low-spin/high-spin equilibrium for Co^{III}, from thermal equilibrium between $\{(OEB)Co^{III}\}$ ($S = 0$) and $\{(OEB^{\bullet})Co^{II}\}$, where $OEB^{\bullet}$ is the oxidized ligand radical dianion, or from temperature dependent coupling of ligand and metal spins in $\{(OEB^{\bullet})Co^{II}\}$. Spectral data indicate that {(OEB)Co] reversibly coordinates pyridine ligands. The manganese(III) complex $\{(OEB)Mn^{III}\}_2$ is dimeric with two helical (OEB)Mn units of like chirality joined by O–Mn bonds to give a dimer of C_2 symmetry. Each manganese ion is five-coordinate, and the magnetic susceptibility is indicative of a high-spin ($S = 2$), d^4 Mn^{III}. In pyridine solution this dimer is cleaved to form monomeric five-coordinate {(OEB)Mn^{III}(py)}. In this complex the maganese ion is coordinated to the four pyrrole nitrogen atoms of the bilindione ligand and to one pyridine ligand.

Introduction

Biliverdins—linear tetrapyrroles that are related to porphyrins—are widely distributed in nature particularly as pigments.[1,2] During heme catabolism, biliverdin IXa, **1**, is formed as a result of oxidative attack upon the α-methine position of heme.[3-5] Coupled oxidation, the oxidation of heme by dioxygen in the presence of a reducing agent in pyridine solution, has been widely adopted as a model for heme catabolism.[6,7] In studies of coupled oxidation of $(py)_2Fe^{II}$(OEP) (OEP is the dianion of octaethylporphyrin), this laboratory has recently shown that an iron complex of the biliverdin (or bilindione) **2** (H_3OEB)[8] is formed along with verdoheme, **3**—the iron(II) complex of octaethyloxaporphyrin,[9] Those results showed that the iron(III) complex of H_3OEB is present in pyridine solution as a monomer, $(py)_2Fe^{III}$(OEB), **4**. This monomeric complex, **4**, undergoes reversible dimerization to form $\{(OEB)Fe^{III}\}_2$, **5**, when pyridine is removed as shown in eq 1.[8]

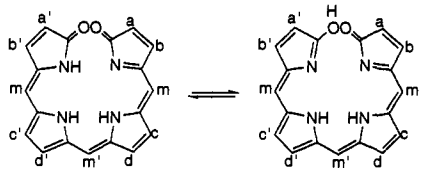

1; a, c, c', b' = methyl; b, a' = vinyl; d,d' = propionate; m,m' = H.
2; a-d' = ethyl m,m' = H; H_3OEB.

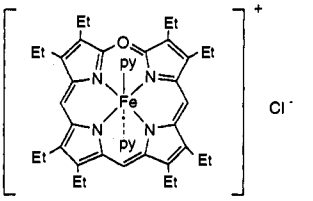

3

The coordination chemistry of the bilindione class of tetrapyrroles has received relatively little attention,[10-12] although Bonnett and co-workers have shown that H_3OEB is a good ligand and

* Abstract published in *Advance ACS Abstracts*, September 1, 1994.

(1) Fox, H. M.; Vevers, G. *The Nature of Animal Colors*; MacMillan Co.: New York, 1960; p 102.
(2) McDonagh, A. F. In *The Porphyrins*; Dolphin, D., Ed.; Academic Press: New York, 1979; Vol. 6, p 293.
(3) O'Carra, P. In *Porphyrins and Metalloporphyrins*; Smith, K. M., Ed.; Elsevier: New York, 1975; p 123.
(4) Schmid, R.; McDonagh, A. F. In *The Porphyrins*; Dolphin, D., Ed.; Academic Press: New York, 1979; Vol. 6, p 257.
(5) Bissell, D. M. In *Liver: Normal Function and Disease. Bile Pigments and Jaundice*; Ostrow, J. D., Ed.; Marcel Decker, Inc.: New York, 1986; Vol. 4, p 133.
(6) Warburg, O.; Negelein, E. *Chem. Ber.* **1930**, *63*, 1816.
(7) Lemberg, R. *Rev. Pure Appl. Chem.* **1956**, *6*, 1.
(8) Balch, A. L.; Latos-Grażyński, L.; Noll, B. C.; Olmstead, M. M.; Safari, N. *J. Am. Chem. Soc.* **1993**, *115*, 9056.
(9) Balch, A. L.; Latos-Grażyński, L.; Noll, B. C.; Olmstead, M. M.; Szterenberg, L.; Safari, N. *J. Am. Chem. Soc.* **1993**, *115*, 1422.
(10) Fuhrhop, J.-H.; Salek, A.; Subramanian, J.; Mengersen, C.; Besecke, S. *Liebigs Ann. Chem.* **1975**, 1131.
(11) Bonnett, R.; Buckley, D. G.; Hamzetash, D. *J. Chem. Soc., Perkin Trans. 1* **1981**, 322.
(12) Bonfiglio, J. V.; Bonnett, R.; Buckley, D. G.; Hamzetash, D.; Hursthouse, K. M.; Malik, K. M. A.; McDonagh, A. F.; Trotter, J. *Tetrahedron* **1983**, *39*, 1865.

0002-7863/94/1516-9114$04.50/0

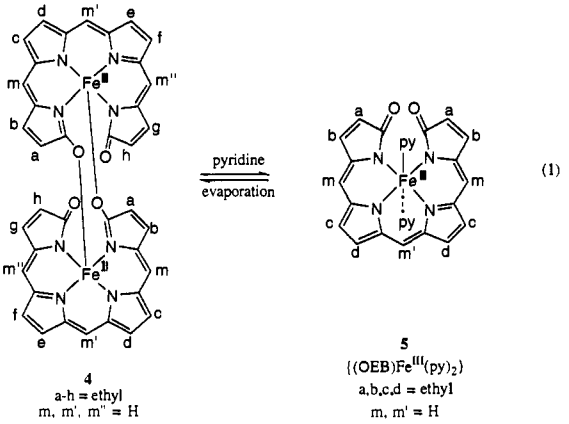

4
a-h = ethyl
m, m', m'' = H

5
{(OEB)Fe^{III}(py)$_2$}
a,b,c,d = ethyl
m, m' = H

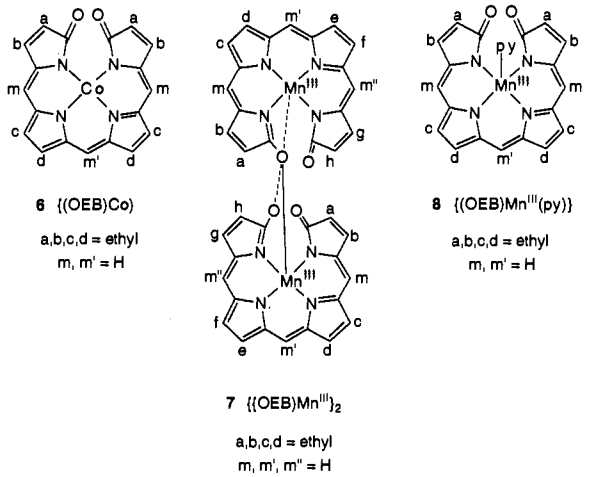

6 {(OEB)Co}
a,b,c,d = ethyl
m, m' = H

7 {(OEB)Mn^{III}}$_2$
a,b,c,d = ethyl
m, m', m'' = H

8 {(OEB)Mn^{III}(py)}
a,b,c,d = ethyl
m, m' = H

that it forms complexes with manganese, cobalt, nickel, copper, and zinc.[11] Because of its ring-opened structure and the presence of two terminal keto groups, this tetrapyrrole cannot readily assume a fully planar geometry and form four bonds of approximately equal length to a central metal ion. Consequently when coordinated, this tetrapyrrole adopts a helical geometry which allows the nitrogen atoms to bind to a centrally placed metal ion while avoiding contact between the keto functions. Crystallographic characterization of a nickel complex of this type has been reported, but the authors noted that the available data did not differentiate between the alternative structures: {(OEBH)-Ni^{II}}, {(OEB)Ni^{III}}, or {(OEB$^{\bullet}$)Ni^{II}}.[12] Thus the state of ligand protonation and the metal and ligand oxidation states were not entirely certain. Recently data regarding the electronic and geometric structure of the copper complex {(OEB$^{\bullet}$)Cu^{II}} have been reported.[13] In this complex, which shows a paramagnetically shifted ^{1}H NMR spectrum but no EPR spectrum in chloroform solution, the ligand is fully deprotonated but is also oxidized so that it acts as a coordinated free radical.

The formation of supramolecular assemblies of ligands into helical superstructures with metal ions as templates has received considerable attention recently.[14] Some linear tetrapyrroles,[15,16] including the bilindione ligand, readily form such helical units. Yet, despite the similarities in the tetrapyrrole ligand backbones, types of different helical structures can result. Here we describe structural results on complexes of cobalt and manganese with the bilindione ligand, **1**. We compare their structures with those of other linear tetrapyrrole ligands.

Results

Synthetic and Spectroscopic Studies. Monomeric {(OEB)Co}, **6**, and dimeric {(OEB)Mn^{III}}$_2$, **7**, were prepared by reaction of H_3OEB with excess cobalt(II) acetate and manganese(II) acetate, respectively, by the procedure reported by Bonnett and co-workers.[11] The cobalt complex **6** is soluble in chloroform and to a lesser extent in dichloromethane to give green solutions which undergo chemical change if exposed to air for several days. Complex **6** is very soluble in pyridine where it forms orange solutions that are very air sensitive. The manganese complex **7** dissolves in chloroform and dichloromethane to form olive-green solutions which are also sensitive to air. Dimeric **7** is very soluble in pyridine, where it gives intense green solutions that are sensitive to air and slowly turn blue.

The UV/vis absorption spectra of the complexes are shown in Figure 1. Trace A shows the spectrum of {(OEB)Co} in chloroform, while trace B shows the same complex in pyridine. The differences between the two spectra suggest that pyridine coordinates the cobalt ion. However, attempts to isolate the presumed pyridine adduct have not been successful. Thus, if pyridine solutions of {(OEB)Co} are evaporated, {(OEB)Co} is recovered. When redissolved in chloroform, the reisolated material gives the spectrum shown in trace A. Solutions of {(OEB)Co} in pyridine are air sensitive, and after several days exposure to air show a new prominent absorption at 668 nm with a second feature with half that intensity at 612 nm. Trace C of Figure 3 shows the UV/vis spectrum of {(OEB}Mn^{III}}$_2$ in chloroform solution, while trace D shows the same complex dissolved in pyridine. Again the spectral differences indicate that pyridine coordinates to the manganese. In this case it is possible to isolate the pyridine cleavage product, {(OEB)Mn^{III}-(py)}, **8**, by addition of *n*-hexane to a pyridine solution of **7**.

Trace A of Figure 2 shows the 300 MHz ^{1}H NMR spectrum of {(OEB)Co} in dichloromethane solution at 23 °C. The pattern of resonances is consistent with the presence of a complex with the helical geometry that is observed in the solid state (*vide infra*). Thus there are two meso resonances, four methyl resonances, and seven methylene resonances, with one with twice the intensity of the other six. Each of the six methylene resonances at lowest field appears as a sextet. Thus each proton within these methylene groups is in a unique environment as is required by the helical nature of the bilindione ligand. At first sight, the spectrum in trace A appears to be that of a typical diamagnetic complex. The lines are narrow, and spin–spin coupling is clearly apparent. Eventually, however, one is struck by the six ppm difference in the positions of the two methine resonances. Such a variation is far greater than what one would expect for a normal, diamagnetic complex. To examine probable causes for this variation, the temperature dependence of the spectrum was examined. Figure 3 shows a plot of the chemical shifts for the meso protons of {(OEB)Co} in tetrachloroethane-d_2, which allows observations over a wider temperature range than dichloromethane but which otherwise shows similar spectral features. These plots are markedly curved with the separation between the meso resonances increasing as the temperature increases. At the lowest temperature the meso resonances occur at 10.5 and 6.6 ppm. Analogous plots for the methylene resonances also show similar, but smaller, curvature. Additionally upon warming, the line widths of all resonances broaden so that at 80 °C in tetrachloroethane-d_2 the spin–spin splitting is obscured. These results are interpreted in terms of a temperature dependent spin-equilibrium. The ground state of the molecule is a singlet, but warming populates an adjacent paramagnetic state. We have examined the possibility that the changes seen in the ^{1}H-NMR spectra are due to changes in the coordination number that result from binding of adventitious ligands. Addition of varying quantities of tetraphenylarsonium chloride to a sample of the complex in

(13) Balch, A. L.; Mazzanti, M.; Noll, B. C.; Olmstead, M. M. *J. Am. Chem. Soc.* **1993**, *115*, 12206.
(14) Constable, E. C. *Angew. Chem., Int. Ed. Engl.* **1991**, *30*, 1450.
(15) Sheldrick, W. S.; Engel, J. *Acta Crystallogr. Sect. B.* **1981**, *B37*, 250.
(16) Struckmeier, G.; Thewalt, U.; Fuhrhop, J.-H. *J. Am. Chem. Soc.* **1976**, *98*, 278.

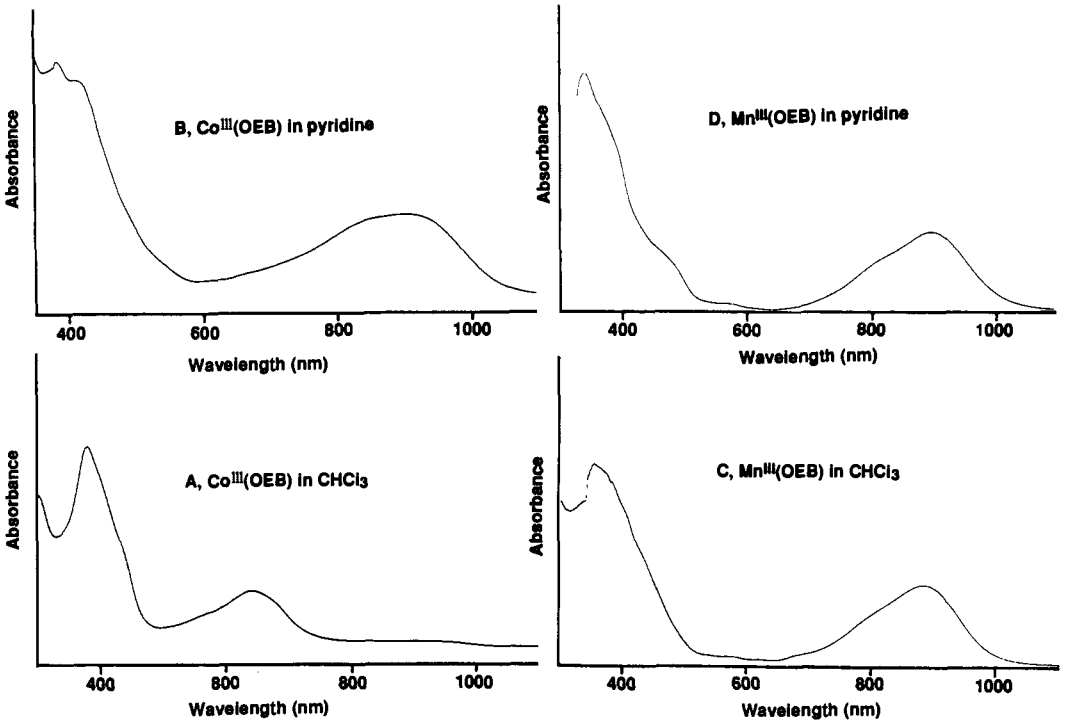

Figure 1. UV/vis absorption spectra of (A) {(OEB)Co} in chloroform solution, λ_{max}, nm (ϵ, M^{-1} cm^{-1}) 642 (1.9×10^4), 380 (6.7×10^4); (B) {(OEB)Co} in pyridine solution, 342 (1.5×10^4), 384 (1.4×10^4), 423 (1.1×10^4), 909 (7.3×10^3); (C) {(OEB)Mn^{III}}$_2$ in chloroform solution, 880 (2.9×10^4), 351 (9.8×10^5); (D) {OEB)Mn^{III}}$_2$ in pyridine solution, 906 (1.2×10^4), 482 (6.9×10^3), 350 (3.5×10^4).

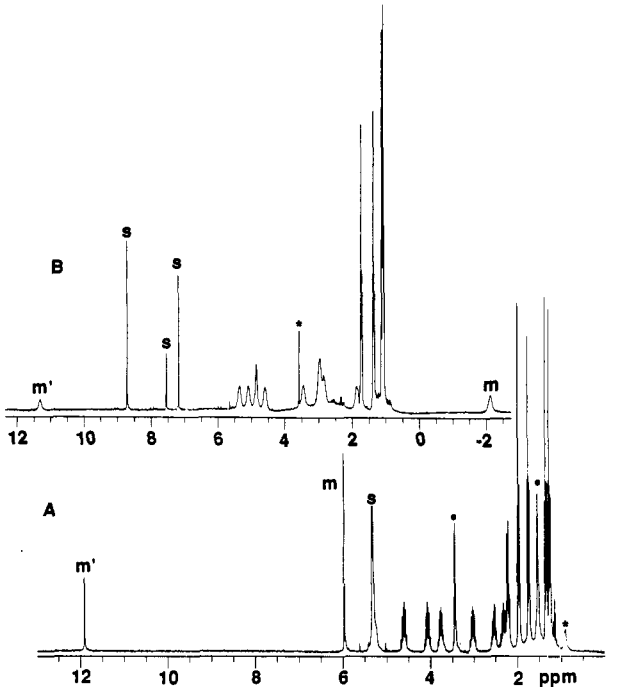

Figure 2. The 300 MHz ^1H NMR spectra of {(OEB)Co} (A) in dichloromethane-d_2 solution at 25 °C and (B) in pyridine-d_5 solution at 30 °C.

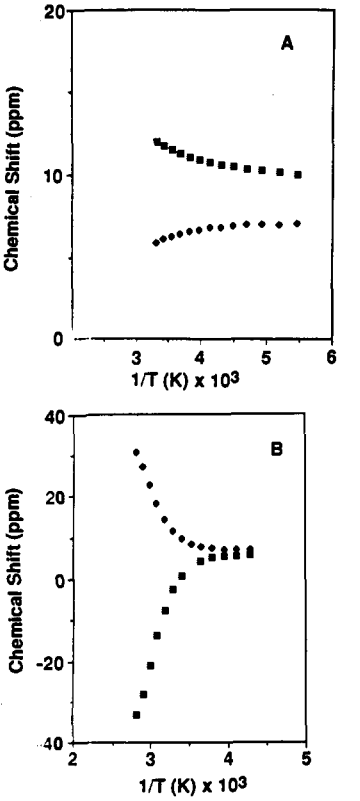

Figure 3. A plot of chemical shift versus $1/T$ for the meso products of {(OEB)Co} in (A) tetrachloroethane-d_2 and (B) pyridine-d_5 solutions.

tetrachloroethane-d_2 solution does not alter the NMR resonances of the complex. Additionally, saturating a solution of the complex with water does not effect the resonances of the complex. We conclude that the temperature dependent spectral changes that are observed do not arise from the addition of ligands to the four-coordinate complex.

The magnetic moment of {(OEB)Co} in the solid state shows temperature dependent changes that are consistent with a spin equilibrium. At 21 °C the magnetic moment is 1.9 μ_β. This value is considerably less than the range of values (2.8–4.5 μ_β) expected for a spin triplet. Upon cooling the moment decreases to 1.6 μ_β at −80 °C and 1.4 μ_β at −173°.

Trace B of Figure 2 shows the ^1H NMR spectrum of {(OEB)-Co} in pyridine-d_5. In comparison with trace A, the lines are all broadened, and the separation between the two meso-resonances is quite large with one shifted downfield and the other far upfield. The effect of temperature on the chemical shift of the meso

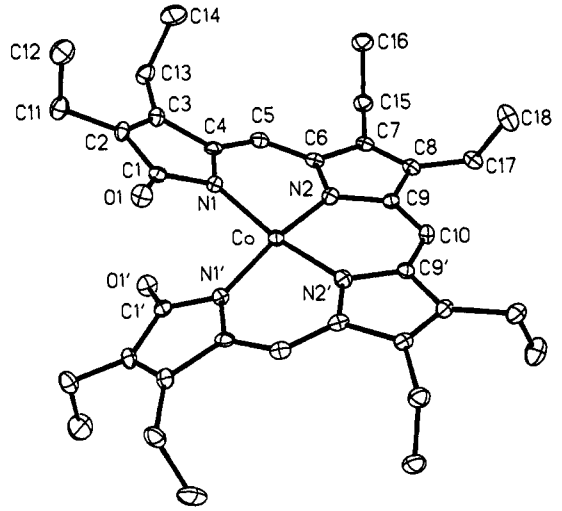

Figure 4. A perspective view of {(OEB)Co} with 50% thermal contours for all non-hydrogen atoms.

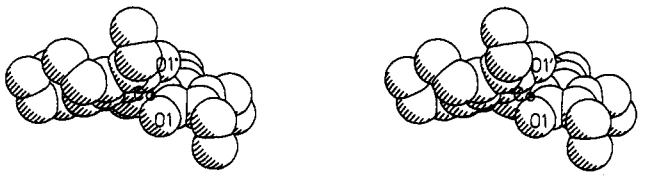

Figure 5. A stereoscopic view of {(OEB)Co} with van der Waals surfaces for the atoms.

resonances is shown in trace B of Figure 3. The curvature of this plot is indicative of a spin state change. At the lowest temperature, however, the two meso resonances occur at 6.3 and 5.8 ppm, and the complex appears to exist in a singlet state. Similar plots for the methylene protons also show curvature.

The infrared spectra of {(OEB)Co} and $\{(OEB)Mn^{III}\}_2$ are reported in the Experimental Section. Neither shows an O–H stretch. For {(OEB)Co} features at 1710 sh and 1683 cm^{-1} are readily assigned to the stretching frequencies of the keto groups. In $\{(OEB)Mn^{III}\}_2$ similar features occur at 1710 and 1672 cm^{-1}.

In chloroform solution $\{(OEB)Mn^{III}\}_2$ has a magnetic moment of 4.7(3) μ_B for each Mn ion. This value is unchanged over the temperature range −50 to +21 °C. This is consistent with the presence of high-spin ($S = 2$), d^4 Mn^{III}. In pyridine solution, where $\{(OEB)Mn^{III}(py)\}$ is formed by cleavage of $\{(OEB)Mn^{III}\}_2$, the magnetic moment at 23 °C is 4.8(3) μ_B for each Mn ion. Again this is consistent with the presence of high-spin, d^4 Mn^{III}. We have not been able to observe an ^1H NMR spectrum for $\{(OEB)Mn^{III}\}_2$. This is not unexpected; Mn^{III} porphyrins are known to exhibit NMR spectra that are characterized by extremely broad lines.[17,18]

The Crystal and Molecular Structure of {(OEB)Co}, 6. This compound has been studied by X-ray diffraction. A perspective view of the complex is shown in Figure 5. Figure 6 shows a stereoscopic view that emphasizes the helical nature of this complex. Table 1 contains selected interatomic distances and angles.

The molecule possess crystallographically imposed C_2 symmetry with the twofold axis passing through the cobalt and the meso (m′) carbon. The cobalt ion is four-coordinate. The Co–N distances (1.873(3), 1.909(3) Å) are similar in length and are shorter than the range of bond lengths (1.95–1.99 Å) found for the Co^{III}–N distances in Co^{III} porphyrin complexes,[19] but these complexes are generally six-coordinate. Cobalt(II) tetraphenylporphyrin, which is four-coordinate, has a Co–N distance of 1.949(3) Å,[20] which is again longer than the Co–N distances in {(OEB)Co}. The apparent shortness of the Co–N distances in {(OEB)Co} may result from the open chain structure of the ligand which allows a degree of radial contraction that is not as possible in a more constrained macrocyclic environment. The C–N and C–C distances within the tetrapyrrole ligand are all normal. The C–O distance (1.209(4) Å) is consistent with the presence of keto functionalities at the ends of the tetrapyrrole. In order to avoid contact between these groups, the ligand has assumed a helical structure in which the two keto functions lie above and below one another. The nonbonded O···O′ separation is 3.116(8) Å. Figure 5 shows the displacements of the core cobalt, carbon, and nitrogen atoms from the mean plane which bisects the molecule and contains the C_2 axis. The out-of-plane displacements are largest at the ends of the tetrapyrrole.

This helical arrangement of the ligand prevents the four pyrrole nitrogen atoms from lying in a common plane and gives the cobalt ion an irregular coordination. Nevertheless, the cis N–Co–N

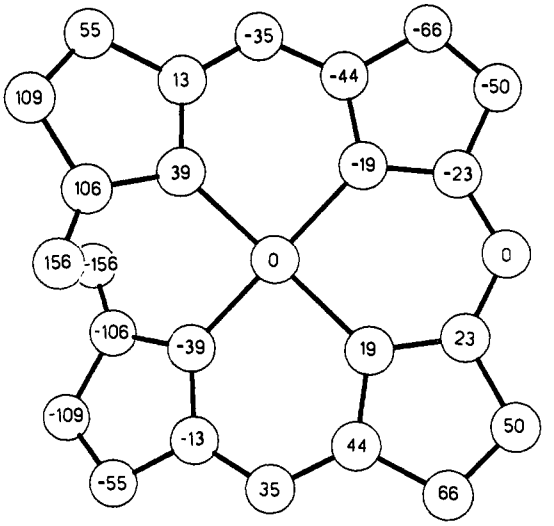

Figure 6. Displacements (in 0.01 Å) of core carbon, oxygen, and nitrogen atoms from the plane which bisects the {(OEB)Co} molecule and which passes through the C_2 axis.

Table 1. Selected Interatomic Distances and Angles for {(OEB)Co}

Distances (Å)			
Co–N(1)	1.873(3)	Co–N(2)	1.909(3)
O(1)–C(1)	1.209(4)	N(1)–C(1)	1.432(5)
N(1)–C(4)	1.366(4)	N(2)–C(6)	1.384(4)
N(2)–C(9)	1.377(4)	C(1)–C(2)	1.490(5)
C(2)–C(3)	1.329(5)	C(5)–C(6)	1.385(5)
C(3)–C(4)	1.486(5)	C(7)–C(8)	1.357(5)
C(4)–C(5)	1.374(5)	C(8)–C(9)	1.451(4)
C(6)–C(7)	1.453(5)	C(9)–C(10)	1.383(4)
C(10)–C(9′)	1.383(4)		
Angles (deg)			
N(1)–Co–N(2)	90.2(1)	N(1)–Co–N(1′)	93.1(2)
N(2)–Co–N(1′)	162.0(2)	N(2)–Co–N(2′)	92.0(2)
Co–N(1)–C(1)	125.6(2)	Co–N(1)–C(4)	128.8(2)
C(1)–N(1)–C(4)	105.6(3)	Co–N(2)–C(6)	126.3(2)
Co–N(2)–C(9)	127.7(2)	C(6)–N(2)–C(9)	105.9(3)
O(1)–C(1)–N(1)	125.3(3)	O(1)–C(1)–C(2)	126.5(4)
N(1)–C(1)–C(2)	108.1(3)	C(1)–C(2)–C(3)	108.0(3)
C(2)–C(3)–C(4)	107.2(3)	N(1)–C(4)–C(3)	110.9(3)
N(1)–C(4)–C(5)	123.8(3)	C(3)–C(4)–C(5)	125.0(3)
C(4)–C(5)–C(6)	122.5(3)	N(2)–C(6)–C(5)	124.1(3)
N(2)–C(6)–C(7)	109.9(3)	C(5)–C(6)–C(7)	125.7(3)
C(6)–C(7)–C(8)	107.0(3)	C(7)–C(8)–C(9)	106.9(3)
N(2)–C(9)–C(8)	110.3(3)	N(2)–C(9)–C(10)	123.9(3)
C(8)–C(9)–C(10)	125.8(3)	C(9)–C(10)–C(9′)	124.4(5)

(17) LaMar, G. N.; Walker, F. A. *J. Am. Chem. Soc.* **1975**, *97*, 5103.
(18) Arasasingham, R. D.; Bruice, T. C. *Inorg. Chem.* **1990**, *29*, 1422.
(19) Arasasingham, R. D.; Balch, A. L.; Olmstead, M. M.; Renner, M. W. *Inorg. Chem.* **1987**, *26*, 3562.
(20) Madura, P.; Scheidt, W. R. *Inorg. Chem.* **1976**, *15*, 3182.

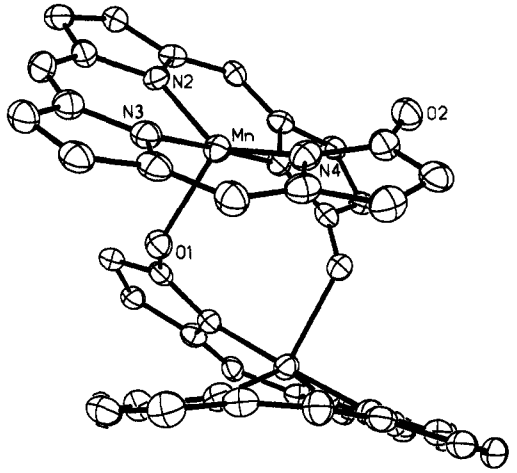

Figure 7. A perspective view of $\{(OEB)Mn^{III}\}_2$ with 50% thermal contours for all non-hydrogen atoms. For clarity the ethyl groups have been omitted.

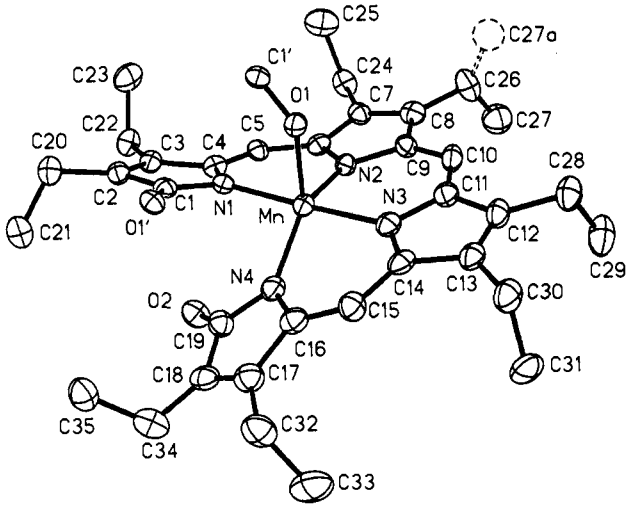

Figure 8. A perspective view of the asymmetric unit and O(1') and C(1') of $\{(OEB)Mn^{III}\}_2$ with 50% thermal contours for all non-hydrogen atoms. One ethyl group is disordered as shown.

angles (90.2(1), 92.0(2), 93.1(2)°), even the N(1)–Co–N(1a) angle which is the widest of these, are near 90°. The trans N(1)–Co–N(2a) angle is 162.0(2)°. Thus the geometry at cobalt must be considered as distorted planar with the distortion resulting from the need to avoid contact between the keto groups at the ends of the tetrapyrrole ligand.

Because of the helicity of the bilindione ligand, each molecule of {(OEB)Co} is chiral. In solution this results in the diastereotopic behavior of each methylene resonance in the ^1H NMR spectrum. However in the crystal, which belong to the space group $C2/c$, there is a center of symmetry which relates pairs of molecules of opposite chirality. Hence, each crystal contains a racemic mixture of the two enantiomers of {(OEB)Co}.

{(OEB)Co} is isostructural with the copper[13] and nickel[12] complexes of the same ligand. However, individual distances within these molecules show some variations.

The Crystal and Molecular Structures of $\{(OEB)Mn^{III}\}_2$·0.1 $CHCl_3$, 7. The results of an X-ray diffraction study are shown in Figures 7 and 8. Table 2 contains selected interatomic distances and angles.

Each $\{(OEB)Mn^{III}\}_2$ molecule consists of two equivalent manganese ions that are coordinated by the two $(OEB)^{3-}$ ligands. These two helical ligands are connected through Mn–O bonds so that the entire ensemble has C_2 symmetry. While each dimeric molecule is therefore chiral, the solid consists of a racemic mixture of the two enantiomers, since in the space group $C2/c$ there is an inversion center which relates a racemic pair of dimers.

Table 2. Selected Bond Lengths and Angles for $\{(OEB)Mn^{III}\}_2$·0.1$CHCl_3$

Bond Lengths (Å)			
Mn–N(1)	1.963(4)	Mn–N(2)	2.020(4)
Mn–N(3)	1.963(4)	Mn–N(4)	1.978(4)
Mn–O(1)	2.105(4)	N(1)–C(1)	1.360(6)
N(1)–C(4)	1.394(6)	N(2)–C(6)	1.355(6)
N(2)–C(9)	1.398(6)	N(3)–C(11)	1.402(6)
N(3)–C(14)	1.361(6)	N(4)–C(16)	1.397(6)
N(4)–C(19)	1.413(7)	O(1)–C(1')	1.256(6)
O(2)–C(19)	1.224(6)	C(1)–C(2)	1.496(7)
C(3)–C(4)	1.469(7)	C(2)–C(3)	1.341(6)
C(4)–C(5)	1.347(6)	C(5)–C(6)	1.425(7)
C(6)–C(7)	1.432(7)	C(7)–C(8)	1.388(7)
C(8)–C(9)	1.435(7)	C(10)–C(11)	1.391(7)
C(9)–C(10)	1.395(7)	C(12)–C(13)	1.377(7)
C(11)–C(12)	1.423(7)	C(15)–C(16)	1.342(8)
C(13)–C(14)	1.448(8)	C(17)–C(18)	1.351(8)
C(14)–C(15)	1.415(7)		
C(16)–C(17)	1.478(8)		
C(18)–C(19)	1.482(7)		
Bond Angles (deg)			
N(1)–Mn–N(2)	89.6(2)	N(1)–Mn–N(3)	177.8(2)
N(2)–Mn–N(3)	90.4(2)	N(1)–Mn–N(4)	93.4(2)
N(2)–Mn–N(4)	143.0(2)	N(3)–Mn–N(4)	87.9(2)
N(1)–Mn–O(1)	89.1(1)	N(2)–Mn–O(1)	98.6(1)
N(3)–Mn–O(1)	88.7(1)	N(4)–Mn–O(1)	118.2(1)
Mn–N(1)–C(1)	125.5(3)	Mn–N(1)–C(4)	126.8(3)
C(1)–N(1)–C(4)	107.6(4)	Mn–N(2)–C(6)	127.2(3)
Mn–N(2)–C(9)	125.5(3)	C(6)–N(2)–C(9)	106.6(4)
Mn–N(3)–C(11)	126.8(3)	Mn–N(3)–C(14)	126.0(3)
C(11)–N(3)–C(14)	106.2(4)	Mn–N(4)–C(16)	123.9(3)
Mn–N(4)–C(19)	129.1(3)	C(16)–N(4)–C(19)	106.1(4)
Mn–O(1)–C(1')	127.4(3)	N(1)–C(1)–C(2)	109.3(4)
C(2)–C(1)–O(1')	125.5(4)	N(1)–C(1)–O(1')	125.2(4)
N(1)–C(4)–C(3)	108.5(4)	C(1)–C(2)–C(3)	106.4(4)
C(3)–C(4)–C(5)	125.7(4)	C(2)–C(3)–C(4)	108.1(4)
N(2)–C(6)–C(5)	123.8(4)	N(1)–C(4)–C(5)	125.3(4)
C(5)–C(6)–C(7)	125.1(4)	C(4)–C(5)–C(6)	124.8(4)
C(6)–C(7)–C(8)	106.6(4)	N(2)–C(6)–C(7)	110.8(4)
C(7)–C(8)–C(9)	106.6(4)	N(2)–C(9)–C(8)	109.4(4)
N(2)–C(9)–C(10)	124.1(4)	C(8)–C(9)–C(10)	126.5(5)
C(9)–C(10)–C(11)	126.1(5)	N(3)–C(11)–C(10)	123.7(5)
N(3)–C(11)–C(12)	109.4(4)	C(10)–C(11)–C(12)	126.7(5)
N(3)–C(14)–C(13)	110.7(4)	C(11)–C(12)–C(13)	107.9(5)
C(13)–C(14)–C(15)	126.3(5)	C(12)–C(13)–C(14)	105.8(4)
N(4)–C(16)–C(15)	124.1(5)	N(3)–C(14)–C(15)	122.8(5)
C(15)–C(16)–C(17)	126.0(5)	C(14)–C(15)–C(16)	124.7(5)
C(16)–C(17)–C(18)	107.5(5)	N(4)–C(16)–C(17)	109.7(4)
C(17)–C(18)–C(19)	107.7(5)	O(2)–C(19)–C(18)	125.2(5)
N(4)–C(19)–O(2)	125.9(5)		
N(4)–C(19)–C(18)	108.9(4)		

The manganese ions are five-coordinate with bonds to four nitrogen atoms of one OEB ligand and to an oxygen of the other OEB ligand. The angular disposition of donors is roughly trigonal bipyramidal with the nearly linear N(2)–Mn–N(3) unit (angle 177.8(2)°) acting as the axis. The Mn, N(2), N(3), O(1) portion is nearly planar. Although the three angles between these ligands show wide variation (N(2)–Mn–N(4), 143.0(2)°; N(4)–Mn–O(1), 118.2(1)°; N(2)–Mn–O(1), 98.6(1)°), their sum is 359.8°. The angles between axial and equatorial donors fall in a much narrower range (88.7–93.4°) that is near the expected 90°. The Mn–N distances to the two axial donors, N(3) and N(1), are of equal length, 1.963(4) Å, and are shorter than the equatorial Mn–N distances Mn–N(2), 2.020(4); Mn–N(4), 1.978(4) Å. For comparison in high-spin Mn^{III} porphyrins, the Mn–N distances fall in the range 1.992–2.072 Å.[19,21,22] The Mn–O distance (2.105(4) Å) is longer than the axial Mn–N distances. This Mn–O distance is similar to that seen in {(OEP)Mn(octaethylporphyrin *N*-oxide)} where the corresponding distance is 2.070(6) Å.[19] The

(21) Tulinsky, A.; Chen, B. M. L. *J. Am. Chem. Soc.* **1977**, *99*, 3647.
(22) Day, V. W.; Stults, B. R.; Tasset, E. L.; Day, R. O.; Marianelli, R. S. *J. Am. Chem. Soc.* **1974**, *96*, 2650.

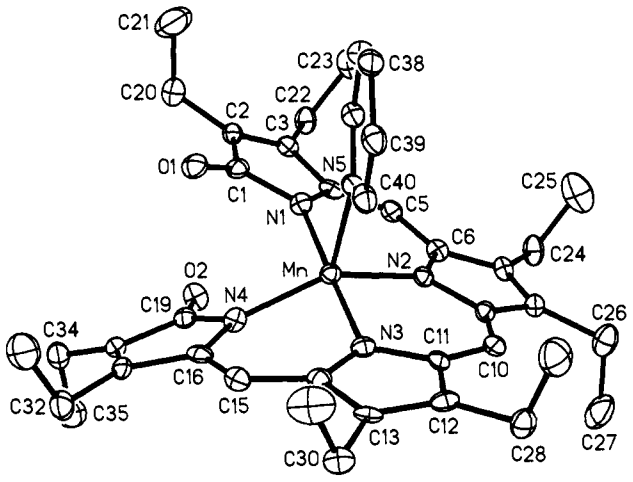

Figure 9. A perspective view of {(OEB)Mn^{III}(py)} with 50% thermal contours for all non-hydrogen atoms.

two manganese ions in **7** are widely separated with a Mn···Mn distance of 4.330(1) Å.

The dimeric structure of {(OEB)Mn^{III}}$_2$ can be viewed as constructed from two monomers of the type seen in {(OEB)Co} by adding two new M–O bonds to connect the monomeric units. This hypothetical addition of the M–O bonds results in folding of one of the formerly trans N–M–N units so that in the dimer of the N(2)–Mn–N(4) angle is 143.0(2)° whereas in {(OEB)Co} the two trans N–Co–N angles are wider, 162.0(2)°. However, in {(OEB)Mn^{III}}$_2$ the other trans angle, N(1)–Mn–N(3), is more nearly linear (177.8(2)°). Thus the formation of the five-coordinate structure for each manganese ion in this dimer requires minor reorganization of the components that are present in a monomer such as {(OEB)Co}.

The Crystal and Molecular Structure of {(OEB)Mn^{III}(py)}, 8. This structure of this five-coordinate monomer as obtained from an X-ray diffraction study is shown in Figure 9. Table 3 contains selected interatomic distances and angles.

The structure of this monomer is similar to the structure of the individual components in {(OEB)Mn^{III}}$_2$. The manganese ion is five-coordinate, and the tetrapyrrole ligand has the helical arrangement that is seen in {(OEB)Mn^{III}}$_2$. The coordination geometry for manganese is that of a distorted trigonal prism. The N(1)–Mn–N(3) unit (bond angle, 177.1(2)°) forms the axis, while the pyrrole nitrogen atoms, N(2) and N(3), and the pyridine nitrogen atom, N(5), lie in the equatorial plane. As with {(OEB)-Mn^{III}}$_2$ the portion consisting of Mn, N(2), N(4), and N(5) is nearly planar with the sum of the angles between these three donors being 359.8°, while there is wide variation in the individual angles which range from 99.8(1) to 142.8(2)°. On the other hand, the six N_{ax}–Mn–N_{eq} angles span a smaller range (93.9-(2)–87.5(2)°) that is near the ideal of 90°. The axial Mn–N distances (Mn–N(1), 1.933(4), Mn–N(3), 1.961(4) Å) are shorter than the equatorial Mn–N distances (Mn–N(2) 1.993(3), Mn–N(4), 1.974(4); Mn–N(5), 2.278(4) Å). Notice that the pyridine N(5)–Mn distance is much longer, however, than any of the pyrrole N–Mn distances. The two C–O distances (C(1)–O(1), 1.217(4); C(19)–O(2), 1.227(5) Å) are entirely consistent with the presence of keto, not alkoxy, groups at the termini of the tetrapyrrole ligand.

Discussion

The available magnetic, structural, and spectroscopic data, especially the lack of O–H vibrations in the infrared spectra, of these complexes of octaethylbilindione, indicate that the complexes contain either trivalent metal ions and the bilindione trianion or divalent metal ions and the bilindione dianion radical. The formation of uncharged complexes as a result of metalation of H_3OEB with manganese(II) and cobalt(II) acetate implies that an oxidation has occurred. In the case of {(OEB)Mn^{III}}$_2$ the metal ion insertion was conducted in the open atmosphere, and dioxygen may serve as oxidant. For the insertion of cobalt, insertions were conducted both in air and under dioxygen-free conditions. The latter produced a cleaner product. In this case it is possible that the excess cobalt(II) acetate is acting as oxidant via a disproportionation reaction. It should also be noted that it is not uncommon to obtain complexes of tetrapyrroles in which the metal oxidation state in the product is different from that in the starting material.[23-25] Thus treatment of porphyrins with zero valent metal carbonyls yields complexes of divalent metal ions.[23,24] In these cases it has been assumed that the ligand serves as oxidant and that dihydrogen is produced.[25] This also may be occurring in the metalation of H_3OEB.

Table 3. Selected Interatomic Distances and Angles for {(OEB)Mn^{III}(py)}

Bond Lengths (Å)			
Mn–N(1)	1.933(4)	Mn–N(2)	1.993(3)
Mn–N(3)	1.961(4)	Mn–N(4)	1.974(4)
Mn–N(5)	2.278(4)	O(1)–C(1)	1.217(4)
O(2)–C(19)	1.227(5)	N(1)–C(1)	1.408(6)
N(1)–C(4)	1.389(5)	N(2)–C(6)	1.372(5)
N(2)–C(9)	1.393(6)	N(3)–C(11)	1.397(6)
N(3)–C(14)	1.371(5)	N(4)–C(16)	1.398(5)
N(4)–C(19)	1.389(6)	N(5)–C(36)	1.352(8)
N(5)–C(40)	1.340(6)	C(1)–C(2)	1.479(7)
C(2)–C(3)	1.338(5)	C(5)–C(6)	1.418(7)
C(3)–C(4)	1.464(7)	C(7)–C(8)	1.371(7)
C(4)–C(5)	1.365(5)	C(8)–C(9)	1.427(5)
C(6)–C(7)	1.423(5)	C(9)–C(10)	1.377(7)
C(10)–C(11)	1.381(5)	C(11)–C(12)	1.428(7)
C(12)–C(13)	1.375(5)	C(15)–C(16)	1.352(7)
C(13)–C(14)	1.423(7)	C(17)–C(18)	1.336(7)
C(14)–C(15)	1.422(6)	C(18)–C(19)	1.477(5)
C(16)–C(17)	1.472(6)		
Bond Angles (deg)			
N(1)–Mn–N(2)	89.9(1)	N(1)–Mn–N(3)	177.1(2)
N(2)–Mn–N(3)	90.4(1)	N(1)–Mn–N(4)	93.9(2)
N(2)–Mn–N(4)	142.8(2)	N(3)–Mn–N(4)	87.6(2)
N(1)–Mn–N(5)	89.7(2)	N(2)–Mn–N(5)	99.8(1)
N(3)–Mn–N(5)	87.5(2)	N(4)–Mn–N(5)	117.2(1)
Mn–N(1)–C(1)	124.5(3)	Mn–N(1)–C(4)	127.9(3)
C(1)–N(1)–C(4)	106.8(4)	Mn–N(2)–C(6)	127.2(3)
Mn–N(2)–C(9)	126.4(3)	C(6)–N(2)–C(9)	106.4(3)
Mn–N(3)–C(11)	125.0(3)	Mn–N(3)–C(14)	125.0(3)
C(11)–N(3)–C(14)	107.0(4)	Mn–N(4)–C(16)	124.5(3)
Mn–N(4)–C(19)	129.1(3)	C(16)–N(4)–C(19)	105.7(3)
Mn–N(5)–C(36)	120.9(3)	Mn–N(5)–C(40)	122.8(4)
C(36)–N(5)–C(40)	116.2(4)	O(1)–C(1)–N(1)	124.9(5)
O(1)–C(1)–C(2)	127.0(4)	N(1)–C(1)–C(2)	108.0(3)
C(1)–C(2)–C(3)	107.9(4)	C(2)–C(3)–C(4)	108.0(4)
C(3)–C(2)–C(20)	130.6(4)	N(1)–C(4)–C(5)	123.9(5)
N(1)–C(4)–C(3)	109.2(3)	C(4)–C(5)–C(6)	125.5(4)
C(3)–C(4)–C(5)	126.8(4)	N(2)–C(6)–C(7)	109.9(4)
N(2)–C(6)–C(5)	122.9(3)	C(6)–C(7)–C(8)	107.4(3)
C(5)–C(6)–C(7)	127.2(4)	N(2)–C(9)–C(8)	109.3(4)
C(7)–C(8)–C(9)	107.0(4)	C(8)–C(9)–C(10)	127.5(4)
N(2)–C(9)–C(10)	123.2(3)	N(3)–C(11)–C(10)	122.7(4)
C(9)–C(10)–C(11)	126.6(4)	C(10)–C(11)–C(12)	128.1(4)
N(3)–C(11)–C(12)	108.8(3)	C(12)–C(13)–C(14)	107.6(4)
C(11)–C(12)–C(13)	107.1(4)	N(3)–C(14)–C(15)	122.5(4)
N(3)–C(14)–C(13)	109.5(3)	C(14)–C(15)–C(16)	124.8(4)
C(13)–C(14)–C(15)	127.9(4)	N(4)–C(16)–C(17)	109.6(4)
N(4)–C(16)–C(15)	123.4(4)	C(16)–C(17)–C(18)	107.4(3)
C(15)–C(16)–C(17)	126.6(4)	O(2)–C(19)–N(4)	125.5(4)
C(17)–C(18)–C(19)	107.5(4)	N(4)–C(19)–C(18)	109.6(4)
O(2)–C(19)–C(18)	124.9(4)		

Coordination by Helical $(OEB)^{3-}$ Ligands. These structural studies show that OEB can bind metal ions in two ways. It can

(23) Tsutsui, M.; Ichikawa, M.; Vohwinkel, F.; Suzuki, K. *J. Am. Chem. Soc.* **1966**, *88*, 854.
(24) Tsutsui, M.; Velapoldi, R. A.; Suzuki, K.; Vohwinkel, F.; Ichikawa, M.; Koyano, T. *J. Am. Chem. Soc.* **1969**, *91*, 6262.
(25) Ostfeld, D.; Tsutsui, M. *Acc. Chem. Res.* **1974**, *7*, 52.

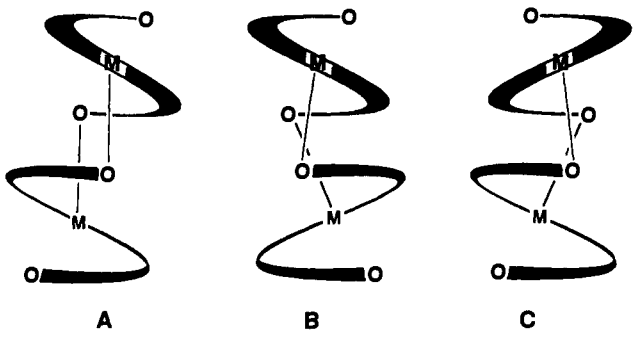

Figure 10. Schematic structures of (A) centrosymmetric $\{(OEB)M^{III}\}_2$ and (B) and (C) the enantiomeric pair of C_2 isomers of $\{(OEB)M^{III}\}_2$.

form a four-coordinate monomer in which the four pyrrole nitrogen atoms act as donors as seen in {(OEB)Co}, or it can form a dimeric structure with five-coordinate metal ions as seen for $\{(OEB)Mn^{III}\}_2$. In both cases the OEB ligand assumes a helical arrangement that allows the terminal keto or alkoxo substituents to avoid contact with one another.

The dimeric structure for $\{(OEB)Mn^{III}\}_2$ is particularly significant because of its relationship to that of $\{(OEB)Fe^{III}\}_2$. The latter has been identified as a product of the coupled oxidation process and characterized in part by an X-ray diffraction study. However, the crystals used in that study suffered from loss of iron from the complex, and the two iron sites exhibited only partial occupancy. This loss of iron from $\{(OEB)Fe^{III}\}_2$ is consistent with its chemical behavior, since the complex readily reacts with water to form free H_3OEB. In the case of $\{(OEB)Mn^{III}\}_2$ there is no sign of loss of manganese ion, and the complex is stable in the presence of water. In the crystal used for data collection, refinement showed full occupancy of the manganese site.

Despite the similarites between $\{(OEB)Mn^{III}\}_2$ and the proposed structure for $\{(OEB)Fe^{III}\}_2$, the two are not identical. When two helical units, (OEB)M, are connected to form a dimer, $\{(OEB)M\}_2$, there are two options. If the two monomeric units that combine have opposite helicity (opposite chirality), then the resulting dimer will be centrosymmetric (and hence achiral) as shown in A of Figure 10. This is the structure proposed for $\{(OEB\}Fe^{III}\}_2$ based on the crystallographic data. However, if the two monomeric units that combine have the same helicity then a chiral dimer with C_2 symmetry will form. The enantiomeric pair of two C_2 dimers is shown as B and C of Figure 10. $\{(OEB)Mn^{III}\}_2$ has this C_2 structure in the solid state. It remains to be seen how stable these dimeric structures are and how readily they interconvert. Nevertheless, it is clear that both the dimeric structures for the iron and manganese complexes can easily be disrupted at the M–O bonds by the addition of a suitable ligand like pyridine.

These dimeric structures also can be contrasted to the dimeric structures that have been formed from other linear tetrapyrroles—formylbiliverdin, **9**,[16] and decamethylbiladien-a,c, **10**.[15]

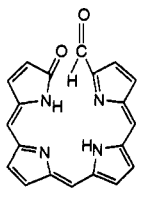

9

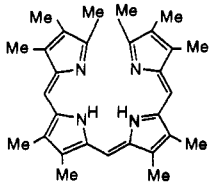

10

While these linear tetrapyrroles have much in common with H_3OEB, they form dimeric structures of a different type, **11**. In these dimers two adjacent pyrrole rings bind to one metal ion, while the other two rings bind to a second metal ion. The dimeric structure is completed by a second tetrapyrrole with similar coordination. The resulting pair of tetrapyrrole helical units are

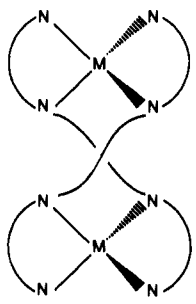

11

entwined to give a dimer with C_2 symmetry. In these each metal ion has tetrahedral geometry.

Electronic Structural Aspects. The electronic structure of complexes of octaethylbilindione are of special interest because of the questions of ligand protonation state and the apparent ease of oxidation of this ligand. For the complexes described here, it is apparent that the ligand is present in the fully deprotonated form.

The electronic structure of the four-coordinate cobalt complex, which we have nominally formulated as {(OEB)Co}, is remarkable. The structural data indicate that the cobalt ion has an approximately planar geometry with Co–N distances that are appropriate for Co^{III}. However, all of the other known planar, four-coordinate cobalt(III) complexes have triplet ground states.[26-31] Additionally, the ^1H NMR spectrum of {(OEB)Co} in poorly coordinating chlorinated hydrocarbon solvents shows temperature dependent shifts (Figure 3) and line broadening that indicate that there is thermal population of a low lying, paramagnetic state. This state could be a metal-based triplet. The metal-based triplet possibility is reasonable since other planar Co^{III} complexes have triplet ground states. Alternately, the complex may be formulated as $\{Co^{II}(OEB^{\bullet})\}$ with a reduced, paramagnetic cobalt ion and an oxidized ligand, which is present as a coordinated radical. Temperature variations in the coupling between the two paramagnetic centers could produce the changes that are seen in the magnetic properties. Finally there may be a thermal equilibrium between a diamagnetic $\{(OEB\}Co^{III}\}$ state and a paramagnetic $\{Co^{II}(OEB^{\bullet})\}$ state. Notice that in the copper complex of the same ligand system, the structure and magnetic properties favor the presence of a $(OEB^{\bullet})Cu^{II}$ rather than a $(OEB)Cu^{III}$ ground state.[13] If Co^{III} is less oxidizing than Cu^{III} in this ligand system, then a ground state formulation as $\{(OEB)Co^{III}\}$ with a nearby $\{(OEB^{\bullet})Co^{II}\}$ state is reasonable.

For the manganese complexes, the magnetic data indicate that high-spin Mn^{III} is present in both dimeric $\{(OEB)Mn^{III}\}_2$ and in monomeric $\{(OEB)Mn^{III}(py)\}$. For the dimer, we did not detect any measurable variation in the magnetic moment in solution over the temperature range −50 to +21 °C. Hence it appears that any magnetic coupling between the two metal ions is small. Since the nonbonded Mn···Mn distances is large, 4.430(1) Å, and the covalent path between the two metal centers is long, this is not unexpected.

Relationships between Complexes of Octaethylbilindione and Octaethyloxophlorin. The linear tetrapyrrole, H_3OEB, and the cyclic tetrapyrrole, octaethyloxophlorin, H_2OEPOH, **12**, share a number of features in their structures and in the fashions in which each coordinates metal ions. Both contain four nitrogen

(26) Eisenberg, R.; Dori, Z.; Gray, H. B.; Ibers, J. A. *Inorg. Chem.* **1968**, *7*, 741.
(27) Birker, P. J. M. W. L.; Bour, J. J.; Steggerda, J. J. *Inorg. Chem.* **1973**, *12*, 1254.
(28) Dorfman, J. R.; Rao, C. P.; Holm, R. H. *Inorg. Chem.* **1985**, *24*, 453.
(29) Fikar, R.; Koch, S. A.; Millar, M. M. *Inorg. Chem.* **1985**, *24*, 3311.
(30) Collins, T. J.; Richmond, T. G.; Santarsiero, B. D.; Treco, B. G. R. T. *J. Am. Chem. Soc.* **1986**, *108*, 2088.
(31) Brewer, J. C.; Collins, T. J.; Smith, M. R.; Santarsiero, B. D. *J. Am. Chem. Soc.* **1988**, *110*, 423.

Table 4. Crystal Data and Data Collection Parameters

	{(OEB)Co}	{(OEB)Mn^{III}}$_2$·0.1$CHCl_3$	{(OEB)Mn^{III}(py)}
formula	$C_{35}H_{43}CoN_4O_2$	$C_{70.1}H_{86.1}Cl_{0.3}Mn_2N_8O_4$	$C_{40}H_{48}MnN_5O_2$
fw	610.7	1225.2	685.8
color and habit	dark needles	dark block	dark parallelepiped
crystal system	monoclinic	monoclinic	triclinic
space group	$C2/c$	$C2/c$	$P\bar{1}$
a, Å	14.645(5)	18.920(4)	11.013(2)
b, Å	18.431(3)	23.067(5)	13.090(3)
c, Å	13.064(4)	16.567(3)	14.710(5)
α, deg	90	90	113.74(2)
β, deg	118.40(2)	98.99(3)	96.84(2)
γ, deg	90	90	105.69(2)
V, Å^3	3102.2(14)	7142(4)	1805.2(8)
T, K	123(2)	123(2)	130(2)
Z	4	4	2
d_{calcd}, g cm^{-3}	1.307	1.140	1.262
radiation, λ(Å)	Cu Kα (1.54178)	Cu Kα (1.54178)	Mo Kα (0.71073)
μ mm^{-1}	4.626	3.362	0.407
range of transm factors	0.80–0.86	0.80–0.89	0.94–0.98
no. data collected	2443	10030	4754
no. unique data	1911	4390	4754
no. data refined	1540	3019	3408
no. parameters	191	382	433
R^a	0.044	0.054	0.050
$R_w{}^b$	0.045[c]	0.062[d]	0.041[e]

[a] $R = \Sigma\|\|F_o\| - \|F_c\|\|/\Sigma|F_o|$. [b] $R_w = \Sigma\|\|F_o\| - \|F_c\|\|w^{1/2}/\Sigma|F_o|w^{1/2}$. [c] $w^{-1} = \sigma^2(F) + 0.0014F^2$. [d] $w^{-1} = \sigma^2(F) + 0.0081F^2$. [e] $w^{-1} = \sigma^2(F) + 0.0001F^2$.

atoms that can act as donors, both have peripheral oxygen atoms that can also act as donors, and both have three protons that can be removed to form trianionic ligands. With trivalent metal ions

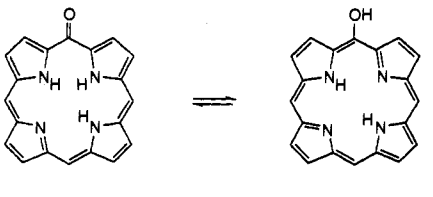

12. H_2OEPOH

these ligand systems are able to form dimeric, five-coordinate complexes in which the peripheral oxygen atoms serve as bridges. The dimeric structure, **13**, for the oxophlorin ligand requires close

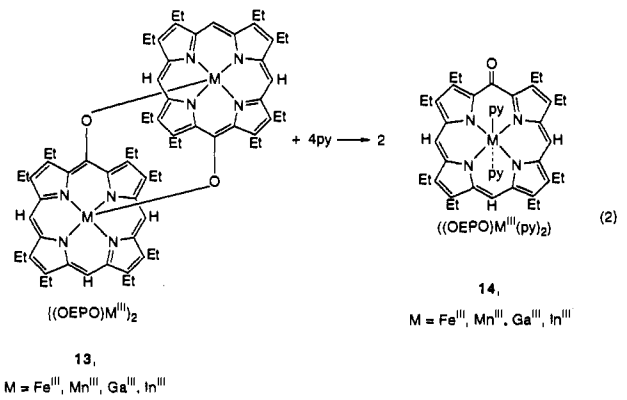

{(OEPO)M^{III}}$_2$

13,
M = Fe^{III}, Mn^{III}, Ga^{III}, In^{III}

14,
M = Fe^{III}, Mn^{III}, Ga^{III}, In^{III}

(2)

approach of the two macrocycles since the cyclic tetrapyrrole maintains a nearly planar geometry and lacks the flexibility of the ring-opened bilindione ligand.[32-34] For both types of dimers, treatment with pyridine readily fragments the dimers to yield five- or six-coordinate pyridine adducts **5**, **8**, or **14** as shown in eqs 1 and 2. In both cases this results in cleavage of the M–O bonds and in the incorporation of the oxygen atoms into peripheral keto groups within the tetrapyrrole ligand. This facile formation of a keto group from an alkoxy ligand is a key feature in allowing the disruption of these dimeric structures in a coordinating solvent such as pyridine.

Additionally H_2OEPOH coordinates divalent metal ions to give four-coordinate complexes with a peripheral hydroxyl group.[35,36] In pyridine solution, these are readily oxidized to form stable radicals. It remains to be seen if the octaethylbilindione ligand system can form analogous complexes, but it should be noted that one other complex, Cu^{II}(OEB$^{\bullet}$), has been recently found to contain the one-electron oxidized bilindione radical dianion.[13] It is also known that oxidation of free H_3OEB yields stable radicals.[10,37]

Experimental Section

Preparation of Compounds. {(OEB)Co}. This was prepared by treatment of H_3OEB with cobalt(II) acetate under a dinitrogen atmosphere according to the procedure of Bonnet and co-workers. Recrystallization was achieved by adding either hexane or methanol to a green dichloromethane solution of the complex. Infrared (ν, cm^{-1} for a hydrocarbon mull): 1710sh, 1683.5, 1651m, 1547m, 1296w, 1139w, 1072m, 1053m, 1012m, 947m, 903w, 871m, 859w, 722m. Crystals suitable for X-ray diffraction were grown by slow evaporation of a dichloromethane/methanol solution of the complex under a dinitrogen atmosphere.

{(OEB)Mn^{III}}$_2$. This was obtained from the reaction of H_3OEB and manganese(II) acetate in air as described by Bonnett and co-workers. Recrystallization was accomplished by addition of hexane to a olive-green chloroform solution of the product. Infrared (ν, cm^{-1} for a hydrocarbon mull): 1710sh, 1672s, 1608s, 1568m, 1546m, 1287w, 1255m, 1191s, 1167w, 1125w, 980m, 915m, 720m. Crystals for the X-ray diffraction study were grown by evaporation of a chloroform/hexane solution of the complex under a dinitrogen atmosphere.

{(OEB)Mn^{III}(py)}. Dark crystals of the complex were obtained by carefully layering dioxygen-free *n*-hexane over a saturated, dioxygen-free pyridine solution that was prepared from **{(OEB)Mn^{III}}$_2$**.

X-ray Data Collection. Crystals of {(OEB)Co} and {(OEB)Mn^{III}}$_2$·0.1$CHCl_3$ were coated with a light hydrocarbon oil and mounted in the 123 K dinitrogen stream of a Siemens P4/RA diffractometer that was equipped with a locally modified LT-2 low temperature apparatus. Intensity data

(32) Balch, A. L.; Noll, B. C.; Olmstead, M. M.; Reid, S. M. *J. Chem. Soc., Chem. Commun.* **1993**, 1088.
(33) Balch, A. L.; Latos-Grażyński, L.; Noll, B. C.; Olmstead, M. M.; Zovinka, E. P. *Inorg. Chem.* **1992**, *31*, 2248.
(34) Balch, A. L.; Noll, B. C.; Reid, S. M.; Zovinka, E. P. *Inorg. Chem.* **1993**, *32*, 2610.
(35) Balch, A. L.; Noll, B. C.; Zovinka, E. P. *J. Am. Chem. Soc.* **1992**, *114*, 3380.
(36) Balch, A. L.; Noll, B. C.; Phillips, S. L.; Reid, S. M.; Zovinka, E. P. *Inorg. Chem.* **1993**, *32*, 4730.
(37) Subramanian, J.; Fuhrhop, J.-H.; Salek, A.; Gossauer, A. *J. Magn. Reson.* **1974**, *15*, 19.

were collected using Ni-filtered CuKα radiation from a Siemens rotating anode X-ray generator that operated at 15 kW. Crystals of {(OEB)-Mn^{III}(py)} were treated similarly and mounted in the cold stream of a Syntex $P2_1$ diffractometer that was equipped with a locally modified LT-1 low temperature apparatus. Intensity data were collected with graphite-monochromated Mo Kα radiation at 130 K. Crystal data are given in Table 4. Two check reflections showed only random (<2%) variation in intensity during data collection. The data were corrected for Lorentz and polarization effects. Further details are given in the supplementary material.

Solution and Structure Refinement. Calculations were performed with SHELXTL Plus v4.2. Scattering factors and corrections for anomalous dispersion were taken from a standard source.[38] Absorption corrections were applied to both structures.[39] Each structure was solved from Patterson maps with subsequent cycles of least square refinement, and calculated difference Fourier maps were used to locate remaining atoms. Hydrogen atoms were fixed to appropriate carbon atoms through the use of a riding model with a fixed isotropic *U*. The structure of {(OEB)-Mn^{III}}$_2$·0.1$CHCl_3$ contained a site which appears to contain a poorly ordered solvent model. This was modeled as 0.1 of a chloroform molecule with four possible chlorine sites.

(38) *International Tables for X-ray Crystallography*; D. Reidel Publishing Co.: Boston, MA, 1992; Vol. C.

(39) Moezzi, B. Ph.D. Thesis, University of California, Davis, CA, 1987.

Acknowledgment. We thank the National Institutes of Health (GM-26226) for financial support and Ms. Tamara N. St Claire for valuable experimental assistance.

Supplementary Material Available: Tables of crystal data, data collection, structure solution and refinement summary, atomic positional parameters, bond distances, bond angles, and anisotropic thermal parameters for {(OEB)Co}, {(OEB)Mn^{III}}$_2$, and {(OEB)-Mn^{III}(py)} (35 pages); tables of observed and calculated structure factors (38 pages). This material is contained in many libraries on microfiche, immediately follows this article in the microfilm version of the journal, and can be ordered from the ACS; see any current masthead page for ordering information.